Differentiation of Niraparib and Olaparib Brain Penetration in a Mouse Brain Metastatic Tumor Model

Abstract #3582

M. Reid Groseclose, Jeremy A. Barry, Tinamarie Skedzielewski, Gerald McDermott, Chakravarthi Balabhadrapatruni, William Benson, Yongle Pang, David Lim, Hoang Tran, Mike Ringenberg, Keyur Gada, Amine Aziez, Elaine Paul, Hasan Alsaid

GSK, Collegeville, PA, USA

Background

- Systemic treatment options for primary and secondary brain tumors remain limited, and outcomes are poor compared with those for extracranial tumors[1]
  - Patients with primary or metastatic brain tumors have poor prognosis and low 5-year survival rates[2]
  - Lack of drug penetration across the blood–brain barrier (BBB) is a key factor[3]
- For the post-radiotherapy treatment of central nervous system tumors, synthetic lethality is an attractive mechanism, but no poly(ADP-ribose) polymerase (PARP) inhibitors are currently approved in this setting[4]
- Recently Sanai et al showed that niraparib reached and maintained pharmacologically relevant concentrations in the brain and glioblastoma tumor tissue, resulting in effective PARP inhibition in patients with newly diagnosed glioblastoma[5]
- In this study, we evaluated the brain penetration and distribution of niraparib and olaparib in organically developed metastatic lesions in a murine brain

Objective

- Evaluate the brain penetration and distribution of 2 PARP inhibitors (niraparib and olaparib) in a murine metastatic brain tumor model

Conclusions

- Niraparib demonstrated higher brain penetration than olaparib in both control mice and those with a metastatic brain tumor; olaparib was not detected in any examined brain sections using matrix-assisted laser desorption/ionization imaging mass spectrometry (MALDI IMS)
- Niraparib demonstrated a significantly higher unbound brain-to-plasma partition coefficient ($K_{p,uu,brain}$) than olaparib; these results are consistent with clinical observations of niraparib crossing into primary brain tumors
- Further studies are warranted to evaluate niraparib as a treatment for primary and metastatic brain tumors

Scan to download a copy of this poster

Presenting author email: reid.x.groseclose@gsk.com

Copies of this e-poster obtained through QR code are for personal use only and may not be reproduced without written permission of the authors.

Presented at the American Association for Cancer Research (AACR) Annual Meeting, April 14–19, 2023; Orlando, FL, USA.

References

1. Hanna C, et al. *Neuro Oncol*. 2020;22(12):1840–1850.
2. Sambade MJ, et al. *Neurooncol Adv*. 2019;1(1):vdz005.
3. Pardridge WM. *Expert Opin Drug Deliv*. 2016;13(7):963–975.
4. Parrish KE, et al. *Mol Cancer Ther*. 2015;14(12):2735–2743.
5. Sanai N, et al. *Neuro Oncol*. 2022;24(7):vii73.

Acknowledgments

This study was funded by GSK (Philadelphia, PA, USA). Writing and editorial support, funded by GSK and coordinated by Hasan Jamal, MSc, of GSK were provided by David M. Jensen, PhD, and Mary C. Wiggin of Ashfield MedComms, an Inizio company.

Conflicts of Interest

All authors are employees of GSK.

Methods

- The study design is summarized in **Figure 1**
- This study was conducted in accordance with the GSK policy on the Care, Welfare, and Treatment of Laboratory Animals and was reviewed by the Institutional Animal Care and Use Committee at GSK
- Female mice (CrTac:NCr-Foxn1nu; 6 weeks old) received 2.5E5 luciferase transfected human breast cancer line (MDA 231-BrM2-831) via intracardiac injection, representing a disrupted BBB model
- Serial tissue sections were collected for MALDI IMS, hematoxylin and eosin (H&E), and immunohistochemistry (IHC) staining from 5 distinct coronal planes in the brain
  - Tissue collected between each imaging plane was homogenized for bioanalysis by liquid chromatography-mass spectrometry (LC-MS)
- Niraparib unbound fractions in plasma and brain homogenate were measured by rapid equilibrium dialysis followed by analysis with LC-MS
- Olaparib unbound fractions in plasma and brain homogenates were cited from literature
- The $K_{p,uu,brain}$, which describes the unbound drug concentration in the brain compared with the blood based solely on the net influx and efflux crossing the BBB, is reported to increase clinical translation

Figure 1. Study Design

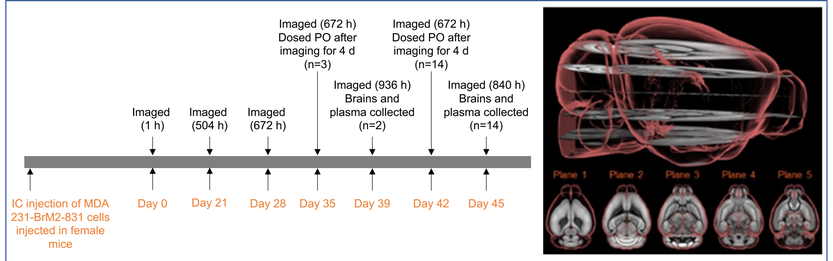

- Model development/BLI
  - Group 1: IC injection of 250,000 cells (MDA 231-BrM-831) in 100 µL of 1× PBS, n=50
  - Group 2: IC stick in left ventricle with no cells, n=10
  - BLI imaging 2× weekly up to 45 d post IC injection
- Dosing (beginning d 35)
  - Mice with BM (n=4) dosed with niraparib (35 mg/kg PO for 4 d)
  - Mice with BM (n=3) dosed with olaparib (50 mg/kg PO for 4 d)
  - Control mice (n=3) dosed with niraparib (35 mg/kg PO for 4 d)
  - Control mice (n=3) dosed with olaparib (50 mg/kg PO for 4 d)
  - Control mice (n=3) vehicle for 4 d
- Tissue collection (2 h after final dose)
  - Terminal plasma (DMPK bioanalysis)
  - Brain (MALDI IMS and DMPK bioanalysis)
    - 5 Horizontal planes from each tissue
      - Sections for MALDI IMS, IHC, H&E, and DMPK

BLI, bioluminescence imaging; BM, brain metastases; DMPK, drug metabolism and pharmacokinetics; H&E, hematoxylin and eosin; IC, intracardiac; IHC, immunohistochemistry; MALDI IMS, matrix-assisted laser desorption/ionization imaging mass spectrometry; PBS, phosphate-buffered saline; PO, orally.

Results

- 16 mice were dosed with niraparib (n=4, brain metastases [BM]; n=3, no BM), olaparib (n=3, BM; n=3, no BM), or vehicle (n=3, control)
- In vivo bioluminescence imaging was used to identify mice with BM (**Figures 2A and 2B**)
  - The presence of human cell-line–derived tumors in the brain was confirmed ex vivo using IHC (**Figures 2C and 2D**)
- The $K_{p,uu,brain}$ was approximately 3-fold and 5.6-fold higher for niraparib than olaparib in BM and no BM mice, respectively (**Table 1**)
  - Olaparib was not detected in any examined brain section
- Quantitative ex vivo imaging analysis by MALDI IMS of brain sections collected from mice administered niraparib showed consistent concentrations distributed throughout the brain parenchyma, with locally higher concentrations detected from tumor regions (**Figures 3 and 4**)
  - Olaparib was not detected by MALDI IMS in BM or no BM mice dosed with that drug (**Figure 3**)
  - H&E-stained sections and MALDI IMS images showed niraparib distribution was nominally higher in the tumor and ventricles than in the parenchyma (**Figure 4**)

Table 1. Drug Concentrations

Drug and mice group	LC-MS bioanalysis		MALDI IMS		
	Terminal plasma,[a] ng/mL	Brain homogenate,[a] ng/g	Brain tumor,[a] ng/g	$K_{p,uu,brain}$[b]	$K_{p,tumor}$[c]
Niraparib					
No BM (n=3)	3847 (595)	658 (71)	—	0.18	0.92
BM (n=4)	2535 (414)	543 (27)	2340 (4057)	0.14	
Vehicle (n=3)	BQL	BQL	—	—	
Olaparib					
No BM (n=3)	226 (75)	6 (5)	—	0.06	NC
BM (n=3)	119 (63)	5 (4)	<LOD	0.03	
Vehicle (n=3)	BQL	BQL	—	—	

[a]Values shown are mean (SD).
[b]Calculated as ratio of mean brain homogenate total concentration adjusted for unbound fraction ($C_{u,brain,ss}$) vs terminal plasma total concentration adjusted for unbound fraction ($C_{u,plasma,ss}$).
[c]Calculated as ratio of mean brain tumor region of interest total concentration vs terminal plasma total concentration.
BM, brain metastasis; BQL, below quantification limit; $K_{p,uu,brain}$, unbound brain-to-plasma partition coefficient; $K_{p,tumor}$, total tumor-to-plasma partition coefficient; LC-MS, liquid chromatography-mass spectrometry; LOD, limit of detection; MALDI IMS, matrix-assisted laser desorption/ionization imaging mass spectrometry; NC, not calculated; SD, standard deviation.

Results *(cont'd)*

Figure 2. In Vivo Bioluminescence Imaging and Ex Vivo IHC

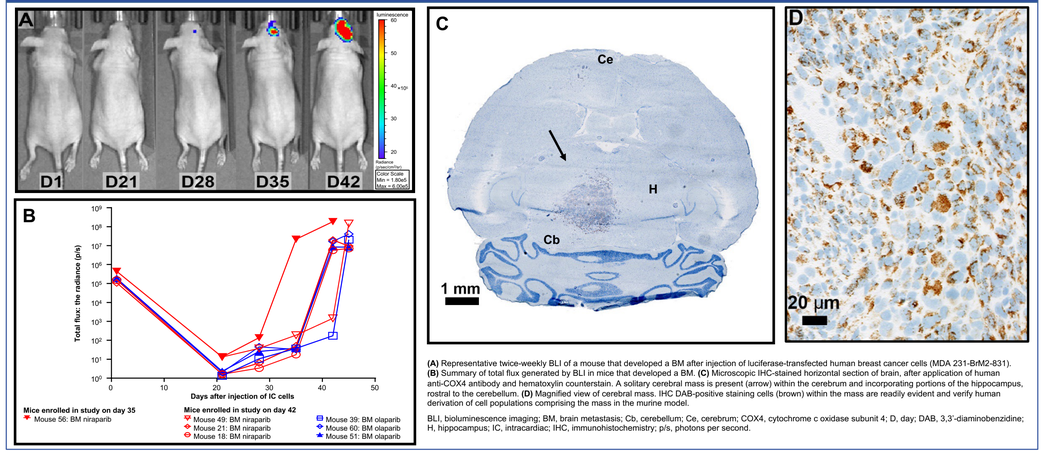

(A) Representative twice-weekly BLI of a mouse that developed a BM after injection of luciferase-transfected human breast cancer cells (MDA 231-BrM2-831). **(B)** Summary of total flux generated by BLI in mice that developed a BM. **(C)** Microscopic IHC-stained horizontal section of brain, after application of human anti-COX4 antibody and hematoxylin counterstain. A solitary cerebral mass is present (arrow) within the cerebrum and incorporating portions of the hippocampus, rostral to the cerebellum. **(D)** Magnified view of cerebral mass. IHC DAB-positive staining cells (brown) within the mass are readily evident and verify human derivation of cell populations comprising the mass in the murine model.

BLI, bioluminescence imaging; BM, brain metastasis; Cb, cerebellum; Ce, cerebrum; COX4, cytochrome c oxidase subunit 4; D, day; DAB, 3,3'-diaminobenzidine; H, hippocampus; IC, intracardiac; IHC, immunohistochemistry; p/s, photons per second.

Figure 3. Brain Penetration and Distribution by MALDI IMS

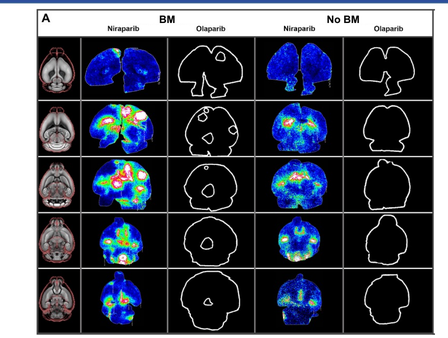

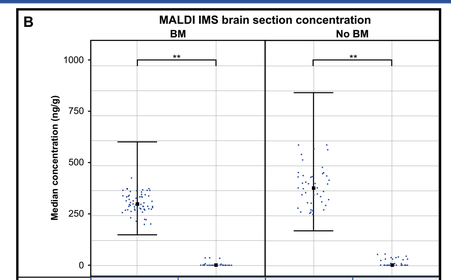

	Niraparib	Olaparib	Niraparib	Olaparib
Mean	314	ND	397	ND
SD	54	—	100	—
Animals (sections)	4 (60)	3 (45)	3 (45)	3 (45)

**P<0.001

(A) MALDI IMS of representative brain tissue sections collected at 5 different anatomical planes from BM mice and no BM mice administered either niraparib or olaparib. **(B)** Above: estimated marginal means (square points) and 95% CIs of the estimated marginal means (error bars) for the concentration of niraparib and olaparib in the BM vs no BM groups. Below: table of the mean, SD, and count of the back-calculated concentrations of niraparib and olaparib in the whole brain.

BM, brain metastases; MALDI IMS, matrix-assisted laser desorption/ionization imaging mass spectrometry; ND, not detected; SD, standard deviation.

Figure 4. Brain Penetration and Distribution of Niraparib in Mice With BM

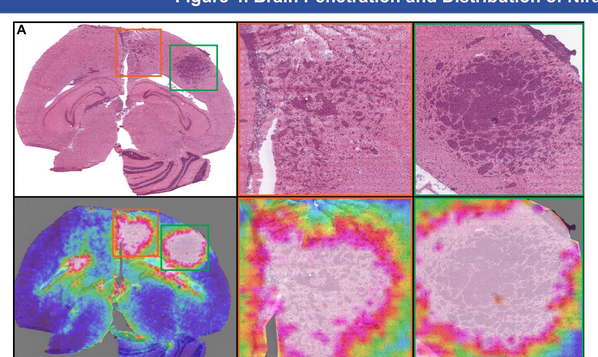

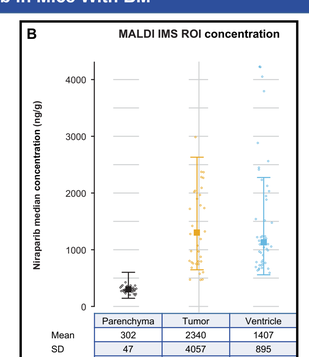

	Parenchyma	Tumor	Ventricle
Mean	302	2340	1407
SD	47	4057	895
Sections	45	45	45

(A) H&E-stained section (above) and MALDI IMS (below) image for niraparib generated from a tissue section collected from a mouse with BM administered niraparib. Magnified view of 2 tumor regions in the mouse brain. **(B)** Summary of localized quantification results generated by MALDI IMS for specific histological regions in the mouse brain plotted as the median concentration detected for each region in all mice with BM administered niraparib.

BM, brain metastases; H&E, hematoxylin and eosin; MALDI IMS, matrix-assisted laser desorption/ionization imaging mass spectrometry; ROI, region of interest; SD, standard deviation.